Available online at www.sciencedirect.com
ScienceDirect
International Journal of Thermal Sciences 47 (2008) 633–640
International Journal of Thermal Sciences
www.elsevier.com/locate/ijts

Local stability analysis of an irreversible Carnot heat engine

Wenjie Nie, Jizhou He *, Xinfa Deng

Department of Physics, Nanchang University, Nanchang 330047, People's Republic of China

Received 6 November 2006; received in revised form 18 April 2007; accepted 18 April 2007

Available online 20 June 2007

Abstract

The local stability of an irreversible Carnot heat engine has been studied based on the linearization technique for dynamical systems and local stability analysis. At two steady-states of the maximum power output and the maximum efficiency the expressions of the relaxation time of an irreversible Carnot heat engine are derived. It is found that the relaxation time is a function of the heat-transfer coefficient α and β, heat capacity C, temperatures of the heat reservoirs T_H and T_L, the degree of internal irreversibility ϕ and the internal heat conductance k. The influence of heat resistance, internal irreversibility and heat leak on the relaxation time is discussed. Phase portraits for the trajectories are presented in some representative cases. The results obtained here are more general and useful for the realistic irreversible heat engine than endoreversible heat engine.

Keywords: Local stability analysis; Irreversible Carnot heat engine; Performance parameters

1. Introduction

In classical thermodynamics, a reversible Carnot heat engine produces the maximum possible work for a given temperatures of the hot and cold reservoirs but generates zero power because it is an infinitely slow operation. The efficiency ($\eta_C = 1 - T_L/T_H$) of Carnot cycle is the upper bound on the efficiency which real heat engine is unrealistically high. In order to seek a more realistic upper bound on the efficiency of a heat engine, Curzon and Ablborn proposed an endoreversible model of Carnot cycle and calculated its efficiency at maximum power output, i.e. so-called CA efficiency $\eta_{\mathrm{CA}} = 1 - \sqrt{T_L/T_H}$ [1]. On the basis of this work, a series of investigations related to endoreversible heat engines have been carried out [2–11].

The endoreversible heat engine requires no internal irreversibility and the sole source of irreversibility is finite-rate heat transfer between the working fluid and the two heat reservoirs. However, real heat engines are usually complex devices with both internal and external irreversibilities. Besides the irreversibility of finite-rate heat transfer, there are also other sources of irreversibility, such as heat leaks, dissipative processes inside the working fluid, and so on. In order to assess the effect of finite-rate heat transfer, together with other major irreversibilities on the performance of heat engines, some new irreversible models of heat engines were established and many significant results were obtained [12–18]. For example, the power versus efficiency relationship for an endoreversible heat engine is a parabolic shaped curve, the behavior of a loop-shaped power versus efficiency appears for a irreversible heat engine, and so on.

Most of the studies of heat engines have focused on their steady-state energetic properties. But the real heat engines are always no-steady and there exists intrinsic cycle variability in the operation of the cycle, for example, incomplete combustion of fuel, friction and other causes. Thus, it is necessary to analyze the effect of noisy perturbations on the stability of system's steady-state. Recently, Santillán et al. studied the local stability of an endoreversible CAN engine working in a maximum power output. L. Guzman-Vargas et al. analyzed the effect of heat transfer laws and thermal conductance on the local stability of an endoreversible heat engine [19,20]. R. Páez-Hernández et al. analyzed the dynamic effects of the time delays and the effect of internal irreversibility on the local stability of non-endoreversible heat engine [21]. Some useful results are obtained. Following their works and taking into account other irre-

* Corresponding author.
E-mail address: hjzhou@ncu.edu.cn (J. He).

1290-0729/$ – see front matter
doi:10.1016/j.ijthermalsci.2007.04.004

Nomenclature

C	heat capacity	W K^{-1}	
F	total surface area of heat exchangers	m^2	
F_1	surface area of the hot-side heat exchanger	m^2	
F_2	surface area of the cold-side heat exchanger	m^2	
J_1	no-steady-state heat flows from warm working fluid to engine	W	
J_2	no-steady-state heat flows from engine to cold working fluid	W	
$\bar{J}_1$	steady-state heat flows from warm working fluid to engine	W	
$\bar{J}_2$	steady-state heat flows from engine to cold working fluid	W	
k	internal conductance of the heat engine	W K^{-1}	
m	temperature ratio of the working fluid		
m_P	optimal temperature ratio of the working fluid at the maximum power output		
m_η	optimal temperature ratio of the working fluid at the maximum efficiency		
P	power output	W	
Q_H	heat transfer supplied by the hot reservoir	W	
Q_L	heat transfer released to the cold reservoir	W	
q	rate of heat leak between the hot and cold reservoirs	W	
T_H	temperature of the hot reservoir	K	
T_L	temperature of the cold reservoir	K	
t	relaxation time	s	
x	temperature of the warm working fluid at no-steady-state	K	
y	temperature of the cold working fluid at no-steady-state	K	
$\bar{x}$	temperature of the warm working fluid at steady-state	K	
$\bar{y}$	temperature of the cold working fluid at steady-state	K	

Greek letters

α	heat transfer coefficient of the hot-side heat exchanger	W K^{-1}
β	heat transfer coefficient of the cold-side heat exchanger	W K^{-1}
η	efficiency	
$\bar{\eta}_0$	efficiency of the irreversible engine without heat leak at steady-state	
ϕ	internal irreversibility factor	
λ	complex number (the eigenvalue)	
τ	temperature ratio of heat reservoirs	

versible factors in heat engines, we further analyze the effect of the heat-transfer coefficient, heat leak and internal irreversibility on local stability of an irreversible Carnot heat engine.

In this paper, we will investigate the local stability of an irreversible Carnot heat engine considering the heat leak and internal irreversibility of engine. Some general results about the local stability analysis of an irreversible heat engine are obtained.

2. An irreversible Carnot engine model

Consider a steady flow Carnot engine model, including the irreversibilities of finite-rate heat transfer between the working fluid and its reservoirs, heat leak between the two reservoirs and internal dissipations of the working fluid, shown in Fig. 1. The working fluid is alternately connected to a hot reservoir at constant temperature T_H and to a cold reservoir at constant temperature T_L, and its temperatures are x and y, respectively. Due to the finite heat transfer, internal dissipations and heat leak, one can derive the expressions of the optimal power output and the optimal efficiency of an irreversible Carnot engine with linear heat transfer law. When the optimal surface area ratio satisfy [16,22]

$$F_1/F_2 = \sqrt{\beta/\phi\alpha} \tag{1}$$

the power output and efficiency are, respectively,

$$P = B\left(1 - \phi m^{-1}\right)(T_H - T_L m) \tag{2}$$

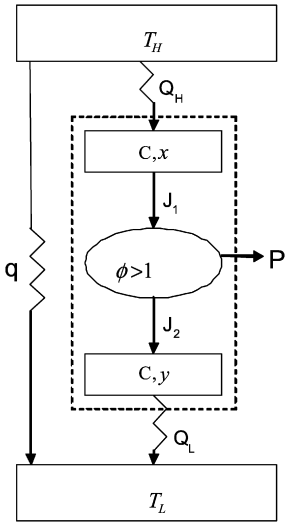

Fig. 1. Schematic diagram of an irreversible Carnot heat engine.

and

$$\eta = \frac{(1 - \phi m^{-1})(T_H - T_L m)}{T_H - T_L m + \rho(T_H - T_L)} \tag{3}$$

where $B = \alpha F/(1 + \sqrt{\phi\alpha/\beta})^2$, $\rho = k/B$, F_1 and F_2 are the surface areas of the hot-side and cold-side heat exchangers, F is the total heat-transfer surface area of the two heat exchangers, α and β are the overall heat-transfer coefficients at the hot- and cold-side heat exchangers, k is the internal heat conductance of the engine, ϕ is the degree of internal irreversibility resulting from internal dissipations of the working fluid, m is

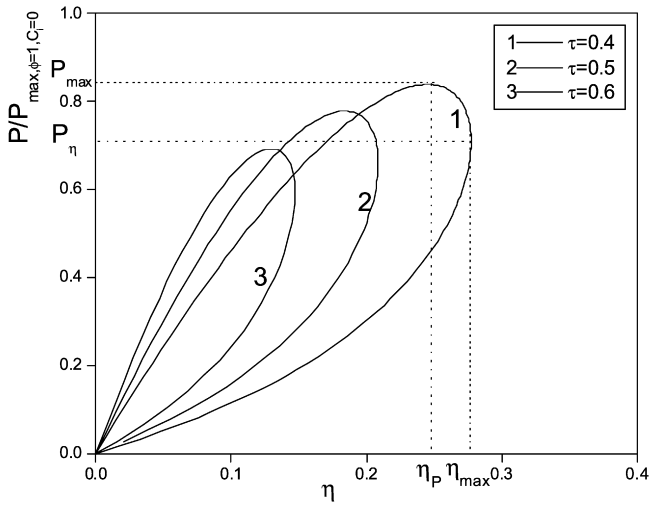

Fig. 2. Plot of power output versus efficiency for different values of τ at given parameters $\phi = 1.1$, $k = 0.2$, $\beta/\alpha = 1$ and $\alpha F = 4$.

the temperature ratio of the working fluid. The characteristic curve of $P \sim \eta$ is a loop shape passing the zero point shown as in Fig. 2. It is clearly shown that there are two steady-state points of the engine. One is a maximum power output $P_{\max}$ and the corresponding efficiency η_P; the other is a maximum efficiency $\eta_{\max}$ and the corresponding power output P_η. Further, one can obtain optimal temperature ratios of the working fluid at the maximum power output ($\mathrm{d}P/\mathrm{d}m = 0$) and the maximum efficiency ($\mathrm{d}\eta/\mathrm{d}m = 0$),

$$m_P = x/y = \sqrt{\phi T_H/T_L} \tag{4}$$

and

$$m_\eta = x/y = (\phi T_H - A)/\left(\phi T_L - qB^{-1}\right) \tag{5}$$

where $A = \sqrt{\phi T_H q B^{-1}(T_H T_L^{-1} - \phi + qB^{-1}T_L^{-1})}$ and $q = k(T_H - T_L)$. The heat flow (Q_H) from the hot reservoir to the warm working fluid through the hot-side heat exchanger and the heat flow (Q_L) from the cold working fluid to the cold reservoir through the cold-side heat exchanger can be expressed as

$$Q_H = \frac{xP}{x - \phi y} \tag{6}$$

and

$$Q_L = \frac{\phi y P}{x - \phi y} \tag{7}$$

3. The steady-state irreversible Carnot engine

Consider the irreversible Carnot engine operates between temperatures $\bar{x}$ and $\bar{y}$, where $\bar{x}$ and $\bar{y}$ represent the steady-state temperatures of working fluid, as shown in Fig. 1. The irreversibility hypothesis means that the cycle is internally irreversible. Thus, the heat flows can be given by

$$\bar{J}_1 = \frac{\bar{x}}{\bar{x} - \phi\bar{y}}\bar{P} \tag{8}$$

and

$$\bar{J}_2 = \frac{\phi\bar{y}}{\bar{x} - \phi\bar{y}}\bar{P} \tag{9}$$

where $\bar{J}_1$ and $\bar{J}_2$ are the steady-state heat flows from $\bar{x}$ to engine and from engine to $\bar{y}$, respectively. $\bar{P}$ is the steady-state power output. The variables with overbars denote steady-state values. When an irreversible Carnot engine operates in a steady-state, this means that the heat flow (Q_H) from T_H to $\bar{x}$ equals to $\bar{J}_1$ and the heat flow (Q_L) from $\bar{y}$ to T_L equals to $\bar{J}_2$, i.e.

$$\bar{J}_1 = \alpha F_1(T_H - \bar{x}) \tag{10}$$

and

$$\bar{J}_2 = \beta F_2(\bar{y} - T_L) \tag{11}$$

According to Eq. (8), the efficiency of an irreversible Carnot engine without heat leak is

$$\bar{\eta}_0 = \bar{P}/\bar{J}_1 = 1 - \phi\bar{y}/\bar{x} \tag{12}$$

It is possible to express temperatures $\bar{x}$ and $\bar{y}$ as

$$\bar{x} = T_H\frac{\sqrt{\phi\alpha/\beta} + \phi\tau(1 - \bar{\eta}_0)^{-1}}{1 + \sqrt{\phi\alpha/\beta}} \tag{13}$$

and

$$\bar{y} = T_L\frac{\sqrt{\alpha/\phi\beta}\,(1 - \bar{\eta}_0)\tau^{-1} + 1}{1 + \sqrt{\phi\alpha/\beta}} \tag{14}$$

where $\tau = T_L/T_H$ is the temperature ratio of heat reservoirs. Using Eqs. (12)–(14) one can obtain the temperatures of the hot and cold reservoirs and power output as a function of $\bar{x}$ and $\bar{y}$

$$T_H = \frac{\sqrt{\phi\alpha/\beta}\,\bar{y}\bar{x} + \bar{y}\bar{x}}{\sqrt{\phi\alpha/\beta}\,\bar{y} + \tau\bar{x}} \tag{15}$$

$$T_L = \frac{\sqrt{\phi\alpha/\beta}\,\bar{y}\bar{x} + \bar{y}\bar{x}}{\sqrt{\phi\alpha/\beta}\,\bar{y}\tau^{-1} + \bar{x}} \tag{16}$$

and

$$\bar{P} = \alpha F_1(\bar{x} - \phi\bar{y})\frac{\bar{y} - \tau\bar{x}}{\sqrt{\phi\alpha/\beta}\,\bar{y} + \tau\bar{x}} \tag{17}$$

4. Local stability analysis of an irreversible Carnot engine

4.1. Linearization and stability analysis [23,24]

Consider the dynamical system

$$\frac{\mathrm{d}x}{\mathrm{d}t} = f(x, y) \tag{18}$$

and

$$\frac{\mathrm{d}y}{\mathrm{d}t} = g(x, y) \tag{19}$$

Let $(\bar{x}, \bar{y})$ be the steady-state solutions of Eqs. (18) and (19) such that $f(\bar{x}, \bar{y}) = 0$ and $g(\bar{x}, \bar{y}) = 0$. If x and y are close to their steady-state values, we can write $x(t) = \bar{x} + \delta x(t)$ and $y(t) = \bar{y} + \delta y(t)$, where $\delta x(t)$ and $\delta y(t)$ are small perturbations. By substituting this into Eqs. (18) and (19) and using the

smallness of $\delta x(t)$ and $\delta y(t)$ to cut at first order in the Taylor series expansions, one can obtain the following set of linear differential equations for perturbations $\delta x(t)$ and $\delta y(t)$:

$$\frac{\mathrm{d}\delta x(t)}{\mathrm{d}t} = f_x \delta x(t) + f_y \delta y(t) \tag{20}$$

and

$$\frac{\mathrm{d}\delta y(t)}{\mathrm{d}t} = g_x \delta x(t) + g_y \delta y(t) \tag{21}$$

where $f_x = (\frac{\partial f}{\partial x})_{\bar{x},\bar{y}}$, $f_y = (\frac{\partial f}{\partial y})_{\bar{x},\bar{y}}$, $g_x = (\frac{\partial g}{\partial x})_{\bar{x},\bar{y}}$ and $g_y = (\frac{\partial g}{\partial y})_{\bar{x},\bar{y}}$. Assume that $\delta x(t)$ and $\delta y(t)$ are of the form

$$\delta x(t) = Z_1 \mathrm{e}^{\lambda t} \tag{22}$$

and

$$\delta y(t) = Z_2 \mathrm{e}^{\lambda t} \tag{23}$$

with λ is a complex number to be determined. Substitution of Eqs. (22) and (23) into Eqs. (20) and (21) leads to the following set of homogeneous linear algebraic equations for Z_1 and Z_2

$$(f_x - \lambda) Z_1 + f_y Z_2 = 0 \tag{24}$$

and

$$g_x Z_1 + (g_y - \lambda) Z_2 = 0 \tag{25}$$

This set of equations has non-trivial solutions only if the determinant of the matrix of coefficients equals zero, i.e.

$$(f_x - \lambda)(g_y - \lambda) - g_x f_y = 0 \tag{26}$$

which is called the characteristic equation and λ is called the eigenvalue. The characteristic relaxation times can be defined as

$$t = \frac{1}{|\lambda|} \tag{27}$$

4.2. Local stability analysis

In order to analyze local stability of an irreversible Carnot heat engine, assuming that the temperatures x and y correspond to macroscopic objects with heat capacity C and are not real heat reservoirs and the working fluid. The heat capacities of the heat reservoirs and the working fluid in two isothermal branches are infinite. Nevertheless, the heat capacity C of the macroscopic objects is finite but large enough. The differential equations for x and y are given by

$$\mathrm{d}x/\mathrm{d}t = \left[\alpha F_1 (T_H - x) - J_1\right]/C \tag{28}$$

and

$$\mathrm{d}y/\mathrm{d}t = \left[J_2 - \beta F_2 (y - T_2)\right]/C \tag{29}$$

where J_1 and J_2 are the heat flows from x to the working substance and from the Carnot engine to y, respectively. By using Eqs. (8) and (9) J_1 and J_2 are given by

$$J_1 = \frac{x}{x - \phi y} P \tag{30}$$

and

$$J_2 = \frac{\phi y}{x - \phi y} P \tag{31}$$

Substitution of Eqs. (30) and (31) into Eqs. (28) and (29) leads to

$$\mathrm{d}x/\mathrm{d}t = \left[\alpha F_1 (T_H - x) - x P/(x - \phi y)\right]/C \tag{32}$$

and

$$\mathrm{d}y/\mathrm{d}t = \left[\phi y P/(x - \phi y) - \beta F_2 (y - T_L)\right]/C \tag{33}$$

4.3. The case of the maximum power output

When the engine works in steady-state of the maximum power output, the optimal temperature ratio of the working fluid is given by Eq. (4)

$$m_P = \bar{x}/\bar{y} = \sqrt{\phi/\tau} \tag{34}$$

The temperature ratio of heat reservoirs τ may be written as a function of $\bar{x}$ and $\bar{y}$

$$\tau = \phi \bar{y}^2/\bar{x}^2 \tag{35}$$

By using Eqs. (12)–(14) and (34), the steady-state values $\bar{x}$ and $\bar{y}$, as function T_L and T_H, can be obtained

$$\bar{x} = T_H \frac{\sqrt{\phi\alpha/\beta} + \sqrt{\phi\tau}}{1 + \sqrt{\phi\alpha/\beta}} \tag{36}$$

and

$$\bar{y} = T_H \frac{\sqrt{\tau\alpha/\beta} + \tau}{1 + \sqrt{\phi\alpha/\beta}} \tag{37}$$

Finally, substituting Eq. (35) into Eq. (17), one can obtain the steady-state power output

$$\bar{P} = \alpha F_1 (\bar{x} - \phi\bar{y})^2 / \left(\sqrt{\phi\alpha/\beta}\,\bar{x} + \phi\bar{y}\right) \tag{38}$$

When the engine works out of the steady-state but not too far away, the power output of an irreversible heat engine depends on x and y in the same way that it depends on $\bar{x}$ and $\bar{y}$ at the steady-state, i.e. $P(x, y) = P(\bar{x}, \bar{y})$. Thus, the dynamic equations for x and y can be obtained by substituting Eq. (38) into Eqs. (32) and (33)

$$\frac{\mathrm{d}x}{\mathrm{d}t} = \frac{\alpha F_1}{C}\left[(T_H - x) - \frac{x(x - \phi y)}{\phi(\sqrt{\alpha/\phi\beta}\,x + y)}\right] \tag{39}$$

and

$$\frac{\mathrm{d}y}{\mathrm{d}t} = \frac{\alpha F_1}{C}\left[\frac{y(x - \phi y)}{\sqrt{\alpha/\phi\beta}\,x + y} - \sqrt{\phi\beta/\alpha}\,(y - T_L)\right] \tag{40}$$

Let $f(x, y)$ and $g(x, y)$ be defined as

$$f(x, y) = \frac{\alpha F_1}{C}\left[(T_H - x) - \frac{x(x - \phi y)}{\phi(\sqrt{\alpha/\phi\beta}\,x + y)}\right] \tag{41}$$

and

$$g(x, y) = \frac{\alpha F_1}{C}\left[\frac{y(x - \phi y)}{(\sqrt{\alpha/\phi\beta}\,x + y)} - \sqrt{\phi\beta/\alpha}\,(y - T_L)\right] \tag{42}$$

After solving the characteristic equation (26), using Eq. (1) and the fact of $F_1 + F_2 = F$, one may get the eigenvalues, i.e.

$$\lambda_{1,2} = -\frac{\alpha F \sqrt{\phi\beta/\alpha}}{2C(\sqrt{\alpha/\beta} + \sqrt{\tau})^2}\left\{\left[\frac{\alpha}{\phi\beta} + \frac{2}{\phi}\sqrt{\frac{\alpha\tau}{\beta}}(\phi + 1) + \tau\right] \pm \sqrt{\Delta_1}\right\} \tag{43}$$

where $\Delta_1 = \tau^2 + \frac{2\alpha}{\beta}[2 + \frac{2}{\phi^2} - \frac{3}{\phi}]\tau + \frac{4\alpha}{\phi^2\beta}\sqrt{\frac{\alpha\tau}{\beta}}(1-\phi) + (\frac{\alpha}{\phi\beta})^2$. By using Eqs. (24) and (25), the corresponding eigenvectors are $u_{1,2} = (1, (1/2\sqrt{\phi})\lfloor\sqrt{\alpha/\beta} + 2(1-\phi)\sqrt{\tau} - \phi\sqrt{\alpha/\beta}(\tau \pm \sqrt{\Delta_1})\rfloor)$, respectively. With the help of the numerical solutions, it is easy to prove that both λ_1 and λ_2 are real and negative ($\lambda_1 < \lambda_2$) for every $0 < \tau < 1$, $\alpha > 0$ and $\beta > 0$. Therefore, the steady-state is stable because any perturbation would decay exponentially with time. The characteristic relaxation times can be obtained

$$t_{1,2} = -1/\lambda_{1,2} \tag{44}$$

i.e.

$$t_{1,2} = \frac{2C(\sqrt{\alpha/\beta} + \sqrt{\tau})^2}{\alpha F\sqrt{\phi\beta/\alpha}}\left\{\left[\frac{\alpha}{\phi\beta} + \frac{2}{\phi}\sqrt{\frac{\alpha\tau}{\beta}}(\phi+1) + \tau\right] \pm \sqrt{\Delta_1}\right\}^{-1} \tag{45}$$

It is shown from Eq. (45) that the heat leak has no any effect for the stability of an irreversible Carnot engine. When the engine is endoreversible, i.e. $\phi = 1$, the values of t_1 and t_2 come back the values of endoreversible CAN engine with liner heat-transfer studied by L. Guazman-Vargas [20].

Relaxation times versus τ are plotted for different values of β/α at a fixed value of $\phi = 1.1$, as shown in Figs. 3(a) and (b). For a given value of $\beta/\alpha < 1$, one can observe that both relaxation times decrease as τ increases, but t_1 is almost constant. The stability improves as $\tau \to 1$. If $\beta/\alpha \to 0$, then $t_2 \to \infty$. The stability of the system is lost. In opposite direction $\beta/\alpha > 1$, t_1 is a decreasing function of τ, but t_2 is not monotonous function of τ and has a minimum value at the special value of τ. As β/α increases both relaxation times decrease.

Relaxation times versus τ are plotted for different values of ϕ at a fixed value of $\beta/\alpha = 1$, as shown in Fig. 4. t_1 increases but t_2 decreases as ϕ increases.

The phase space portrait of $x(t)$ versus $y(t)$ at fixed values of $\beta/\alpha = 1$, $\phi = 1.1$ and $\tau = 0.4$ is shown in Fig. 5. The trajectories approach the origin (steady-state values $\bar{x}, \bar{y}$) tangent to the slow eigendirection corresponding to eigenvector $u_2 = (1, 0.85)$. In backwards time ($t \to -\infty$), the trajectories are parallel to the fast eigendirection corresponding to eigenvector $u_1 = (1, -0.44)$. It is found that both $x(t)$ and $y(t)$ decay exponentially to the origin.

4.4. The case of the maximum efficiency

When the engine works in steady-state of the maximum efficiency, the optimal temperature ratio of the working fluid is given by Eq. (5)

$$m_\eta = \frac{\bar{x}}{\bar{y}} = \frac{\phi - \sqrt{\rho\phi(\tau^{-1}-1)(1+\rho-\rho\tau-\phi\tau)}}{\phi\tau - \rho(1-\tau)} \tag{46}$$

where $\tau \leqslant \tau_{\max} = (1+\rho)/(\phi+\rho)$. From Eq. (46) one can write the temperature ratio τ as a function of $\bar{x}$ and $\bar{y}$,

$$\tau = \left\{\left(\rho\bar{x}^2 + 2\phi\bar{x}\bar{y} + \rho\phi\bar{y}^2\right) - \sqrt{\left(\rho\bar{x}^2 + 2\phi\bar{x}\bar{y} + \rho\phi\bar{y}^2\right)^2 - 4\phi\bar{x}^2\bar{y}^2(1+\rho)(\phi+\rho)}\right\} \Big/ \left\{2(\phi+\rho)\bar{x}^2\right\} \tag{47}$$

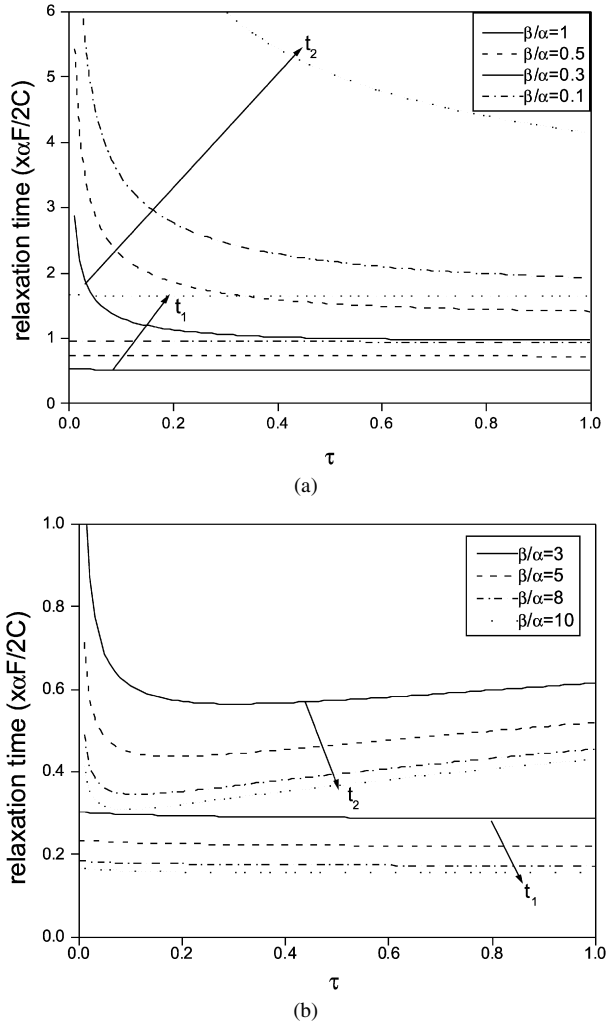

Fig. 3. Plot of relaxation times versus τ for different values of β/α at given parameter $\phi = 1.1$.

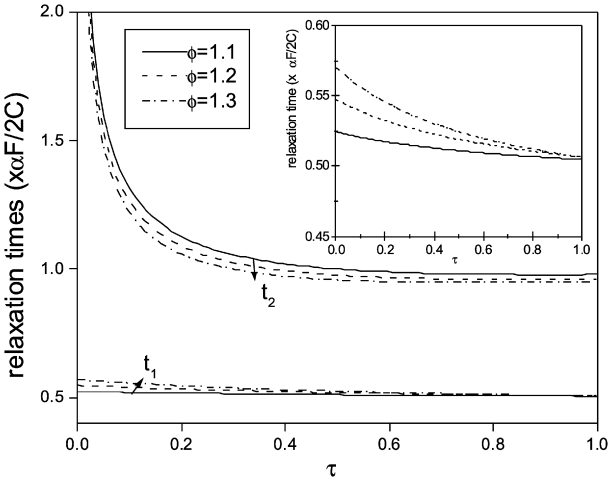

Fig. 4. Plots of relaxation times versus τ for different values of ϕ at given parameter $\beta/\alpha = 1$.

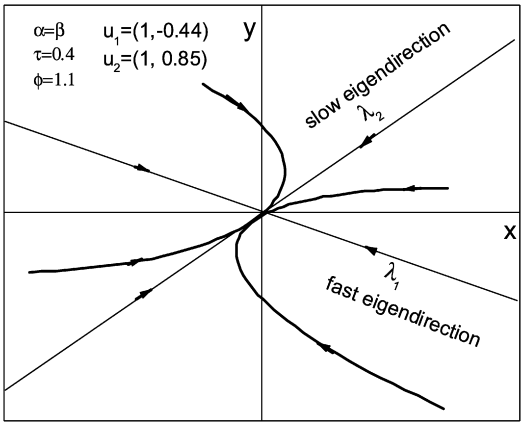

Fig. 5. Qualitative phase space portrait of $x(t)$ versus $y(t)$ at fixed values of $\beta/\alpha = 1$, $\phi = 1.1$ and $\tau = 0.4$ for the case of the maximum power output.

By using Eqs. (12)–(14) and (46), the steady-state values $\bar{x}$ and $\bar{y}$, as function T_L and T_H, can be obtained

$$\bar{x} = T_H\{\phi\tau(1+\sqrt{\phi\alpha/\beta}) + \rho(\tau-1)\sqrt{\phi\alpha/\beta} - \sqrt{\rho\phi\tau(1-\tau)(1+\rho-\rho\tau-\phi\tau)}\} / \{(1+\sqrt{\phi\alpha/\beta})(\phi\tau-\rho+\rho\tau)\} \quad (48)$$

and

$$\bar{y} = T_H\{\phi\tau(1+\sqrt{\phi\alpha/\beta}) + \rho(\tau-1)\sqrt{\phi\alpha/\beta} - \sqrt{\rho\phi\tau(1-\tau)(1+\rho-\rho\tau-\phi\tau)}\} / \{(1+\sqrt{\phi\alpha/\beta}) \times (\phi - \sqrt{\rho\phi(\tau^{-1}-1)(1+\rho-\rho\tau-\phi\tau)})\} \quad (49)$$

By using Eqs. (17), (32), (33) and (47), the dynamic equations for x and y can be obtained

$$\frac{dx}{dt} = \frac{\alpha F_1}{C}\left[T_H - \frac{(1+\sqrt{\phi\alpha/\beta})xy}{\sqrt{\phi\alpha/\beta}\,y + \tau x}\right] \quad (50)$$

and

$$\frac{dy}{dt} = \frac{\alpha F_1}{C}\left[\sqrt{\phi\beta/\alpha}T_L - \frac{(\phi+\sqrt{\phi\beta/\alpha})\tau xy}{\sqrt{\phi\alpha/\beta}\,y + \tau x}\right] \quad (51)$$

where τ is decided by Eq. (47) as long as $\bar{x}$ and $\bar{y}$ are replaced by x and y, respectively. Let $f(x, y)$ and $g(x, y)$ be defined as

$$f(x,y) = \frac{\alpha F_1}{C}\left[T_H - \frac{(1+\sqrt{\phi\alpha/\beta})xy}{\sqrt{\phi\alpha/\beta}\,y + \tau x}\right] \quad (52)$$

and

$$g(x,y) = \frac{\alpha F_1}{C}\left[\sqrt{\phi\beta/\alpha}T_L - \frac{(\phi+\sqrt{\phi\beta/\alpha})\tau xy}{\sqrt{\phi\alpha/\beta}\,y + \tau x}\right] \quad (53)$$

After solving the characteristic equation (26), one may get the eigenvalues, i.e.

$$\lambda_{1,2} = \frac{-\alpha F}{2C(\sqrt{\phi\alpha/\beta}+\tau m_\eta)^2}\left[(b+\sqrt{\phi\alpha/\beta} + \phi b + \tau^2 m_\eta^2\sqrt{\phi\beta/\alpha}) \pm \sqrt{\Delta_2}\right] \quad (54)$$

where

$$\Delta_2 = \left(-b - \sqrt{\phi\alpha/\beta} + \phi b + \tau^2 m_\eta^2\sqrt{\phi\beta/\alpha}\right)^2 + 4\phi(\tau m_\eta - b)^2$$

$$b = \frac{(\rho+m_\eta)\phi}{(\phi+\rho)m_\eta} - \{\phi(m_\eta+\rho)(\rho m_\eta^2 + 2\phi m_\eta + \rho\phi) - 2(\phi+\rho)(1+\rho)\phi m_\eta^2\} / \left\{(\phi+\rho)m_\eta \times \sqrt{(\rho m_\eta^2 + 2\phi m_\eta + \rho\phi)^2 - 4(\phi+\rho)(1+\rho)\phi m_\eta^2}\right\}$$

The corresponding eigenvectors are $u_{1,2} = (1, (\phi b - b - \sqrt{\phi\alpha/\beta} + \tau^2 m_\eta^2\sqrt{\phi\beta/\alpha} \pm \sqrt{\Delta_2})/2m_\eta(m_\eta\tau - b))$, respectively. The characteristic relaxation times are obtained

$$t_{1,2} = \frac{2C(\sqrt{\phi\alpha/\beta}+\tau m_\eta)^2}{\alpha F}\left[(b+\sqrt{\phi\alpha/\beta} + \phi b + \tau^2 m_\eta^2\sqrt{\phi\beta/\alpha}) \pm \sqrt{\Delta_2}\right]^{-1} \quad (55)$$

Eq. (55) is the general expression of the characteristic relaxation times as a function of τ, k, ϕ and β/α. By using numerical solution, it is easy to prove that λ_1 and λ_2 are negative ($\lambda_1 < \lambda_2$) for every $0 < \tau < 1, \alpha > 0, \beta > 0, k > 0$ and $\phi > 1$. Thus, the steady-state of the maximum efficiency is also stable because λ_1 and λ_2 are negative. Every small perturbation around the steady-state values of the temperature of the working fluid would decay exponentially with time.

Relaxation times versus τ are plotted for different values of β/α at given parameters $\phi = 1.1, k = 0.1$ and $\alpha F = 4$, as shown in Figs. 6(a) and (b). For a given value of $\beta/\alpha < 1$, one can observe that the relaxation time t_2 decreases but t_1 increases faintly as τ increases. If $\beta/\alpha \to 0$, then $t_2 \to \infty$. The stability of the system is lost. In opposite direction $\beta/\alpha > 1$, both t_1 and t_2 are not monotonous function of τ. t_1 shows a maximum but t_2 shows a minimum at different value of τ. As β/α increases both relaxation times decrease. It is also shown that τ has the upper bound $\tau_{\max}$.

Relaxation times versus τ are plotted for different values of ϕ at given $\beta/\alpha = 1, k = 0.1$ and $\alpha F = 4$, as shown in Fig. 7. The relaxation time t_1 is not monotonous function of τ. t_2 decreases as τ increases. As ϕ increases t_1 increases but decreases subsequently. t_2 decreases with increasing ϕ. It is worthy to note that ϕ has great influence on the upper bound of τ.

Relaxation times versus τ are plotted for different values of k at given $\beta/\alpha = 1, \phi = 1.1$ and $\alpha F = 4$, as shown in Fig. 8. The relaxation time t_1 is not monotonous function of τ. t_2 decreases as τ increases. As k increases t_1 decreases but t_2 increases.

The phase space portrait of $x(t)$ versus $y(t)$ at fixed values of $\beta/\alpha = 1$, $\phi = 1.1$, $k = 0.2$ and $\tau = 0.4$ is shown in Fig. 9. For the case of maximum efficiency, the trajectories approach the origin (steady-state values $\bar{x}, \bar{y}$) tangent to the slow eigendirection corresponding to eigenvector $u_2 = (1, 0.82)$. In backwards time ($t \to -\infty$), the trajectories are parallel to the fast eigendirection corresponding to eigenvector $u_1 = (1, -0.35)$. It is found that both $x(t)$ and $y(t)$ decay exponentially to the origin.

5. Conclusions

The local stability analysis of an irreversible Carnot engine obeyed by Newton's heat transfer law is presented in this paper. The general expressions of relaxation times for different

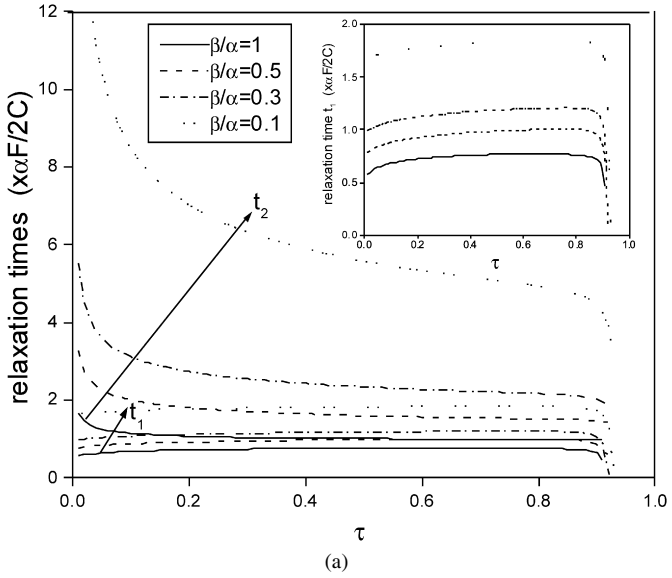

(a)

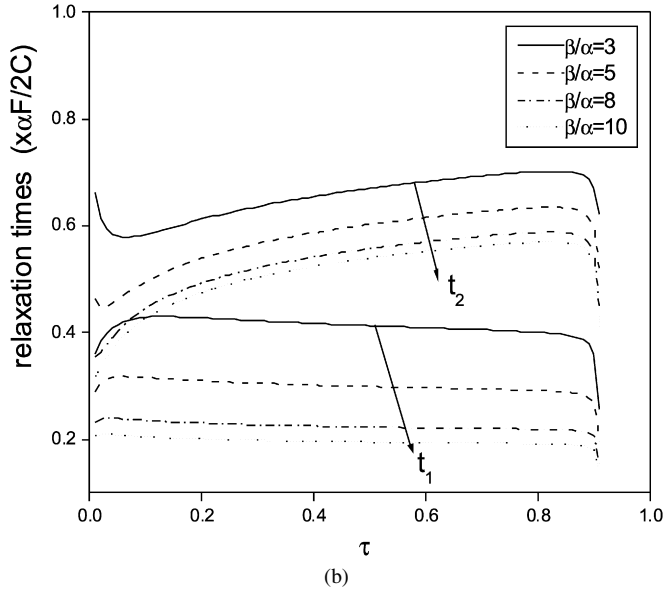

(b)

Fig. 6. Plots of relaxation times versus τ for different values of β/α at given parameters $\phi = 1.1$, $k = 0.1$ and $\alpha F = 4$.

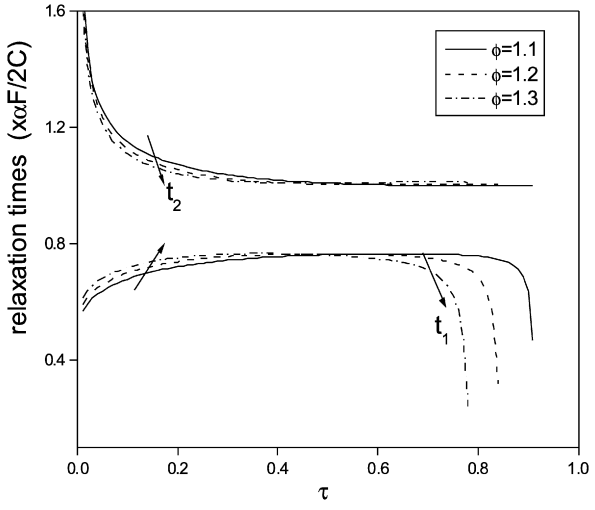

Fig. 7. Plots of relaxation times versus τ for different values of ϕ at given parameters $\beta/\alpha = 1$, $k = 0.1$ and $\alpha F = 4$.

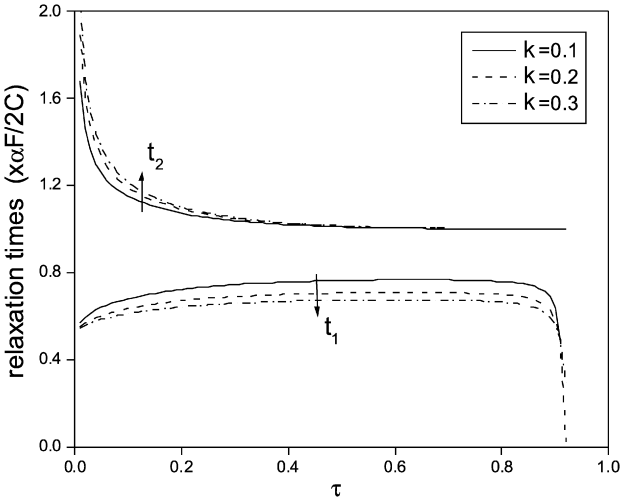

Fig. 8. Plots of relaxation times versus τ for different values of k at given parameters $\beta/\alpha = 1$, $\phi = 1.1$ and $\alpha F = 4$.

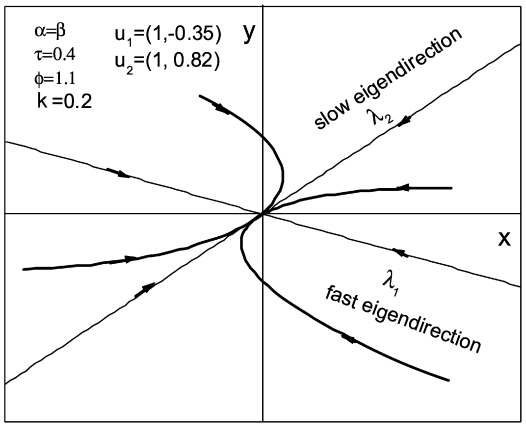

Fig. 9. Qualitative phase space portrait of $x(t)$ versus $y(t)$ at fixed values of $\beta/\alpha = 1$, $\phi = 1.1$, $k = 0.2$ and $\tau = 0.4$ for the case of the maximum efficiency.

steady-state points (the maximum power output or the maximum efficiency) are derived. The influence of heat resistance, internal irreversibility and heat leak on the relaxation time is shown in Figs. 3–4 and 6–8. The phase portraits clearly show that any perturbation on x and y values tend to come back the steady-state and the decay of speed of internal temperature is different. The results obtained here are general and be useful for both determination of optimal operating conditions and design of heat engines.

Acknowledgements

This work was supported by National Natural Science Foundation (No. 10465003), Natural Science Foundation of Jiangxi, People's Republic of China (No. 0412011) and The Science and Technology Foundation of Jiangxi Education Bureau.

References

[1] F.L. Curzon, B. Ahborn, Efficiency of a Carnot engine at maximum power output, Am. J. Phys. 43 (1975) 22–24.

[2] M.H. Rubin, B. Andresen, Optimal staging of endoreversible heat engines, J. Appl. Phys. 52 (1982) 1–7.
[3] A. Bejan, Entropy generation minimization: the new thermodynamics of finite-size devices and finite-time processes, J. Appl. Phys. 79 (1996) 1191–1281.
[4] J.M. Gordon, Maximum power point characteristics of heat engines as a general thermodynamic problem, Am. J. Phys. 57 (1989) 1136–1142.
[5] A. De Vos, Efficiency of some heat engines at maximum power conditions, Am. J. Phys. 53 (1985) 570–573.
[6] A. De Vos, Reflections on the power delivered by endoreversible engine, J. Phys. D: Appl. Phys. 20 (1987) 232–236.
[7] L. Chen, Z. Yan, The effect of heat-transfer law on performance of two-heat-source endoreversible cycle, J. Chem. Phys. 90 (1989) 3740–3743.
[8] C. Wu, Power optimization of a finite time Carnot heat engine, Energy 13 (1988) 681–687.
[9] L.B. Erbay, H. Yavuz, An analysis of an endoreversible heat engine with combined heat transfer, J. Phys. D: Appl. Phys. 30 (1997) 2841–2847.
[10] G. De Mey, A. De Vos, On the optimum efficiency of endoreversible thermodynamic processes, J. Phys. D: Appl. Phys. 27 (1994) 736–739.
[11] J. Chen, C. Wu, Maximum specific power output of a two-stage endoreversible combined cycle, Energy 20 (1994) 305–309.
[12] L. Chen, F. Sun, C. Wu, The influence of internal heat leak on the power versus efficiency characteristics of heat engines, Energy Convers. Mgmt. 38 (1997) 1501–1507.
[13] J.M. Gordon, M. Huleihil, On optimizing maximum-power heat engine, Am. J. Phys. 6 (1991) 1–7.
[14] J.M. Gordon, M. Huleihil, General performance characteristics of real heal engines, J. Appl. Phys. 72 (1992) 829–837.
[15] Z. Yan, L. Chen, Optimal performance of a generalized Carnot cycle for another linear heat transfer law, J. Chem. Phys. 9 (1990) 1994–1998.
[16] L. Chen, F. Sun, C. Wu, A generalized model of real heat engines and its performance, J. Inst. Energy 69 (1996) 214–222.
[17] J. Chen, The maximum power output and maximum efficiency of an irreversible Carnot heat engine, J. Phys. D: Appl. Phys. 27 (1994) 1144–1149.
[18] F. Moukalled, R.Y. Nuwayhid, N. Noueihed, The efficiency of endoreversible heat engines with heat leak, I, J. Energy. Res. 19 (1995) 377–389.
[19] M. Santillan, G. Maya-Aranda, F. Angulo-Brown, Local stability analysis of an endoreversible Curzon–Ahborn–Nouikov engine working in a maximum-power-like regime, J. Phys. D: Appl. Phys. 34 (2001) 2068–2072.
[20] L. Guzman-Vargas, I. Reyes-Ramirez, N. Sanchez, The effect of heat transfer laws and thermal conductances on the local stability of an endoreversible heat engine, J. Phys. D: Appl. Phys. 38 (2005) 1282–1291.
[21] R. Páez-Hernández, F. Angulo-Brown, M. Santillán, Dynamic robustness and thermodynamic optimization in a non-endoreversible Curzon–Ahlborn engine, J. Non-Equilibrium Thermodyn. 31 (2006) 173–188.
[22] L. Chen, F. Sun, C. Wu, Effect of a heat transfer law on the performance of a generalized irreversible Carnot-engine, J. Phys. D: Appl. Phys. 32 (1999) 99–105.
[23] H.S. Strogatz, Non Linear Dynamics and Chaos: With Applications to Physics, Chemistry and Engineering, Perseus, Cambridge, 1994.
[24] S. Lang, Linear Algebra, Springer, New York, 1987.